A decision tree model to predict liver cirrhosis in hepatocellular carcinoma patients: a retrospective study

Zheyu Zhou[1],[*], Chaobo Chen[2],[3],[*], Meiling Sun[3], Xiaoliang Xu[4], Yang Liu[3], Qiaoyu Liu[4], Jincheng Wang[4], Yin Yin[4] and Beicheng Sun[1],[4]

[1] Department of General Surgery, Nanjing Drum Tower Hospital, Chinese Academy of Medical Sciences & Peking Union Medical College, Graduate School of Peking Union Medical College, Nanjing, China
[2] Department of General Surgery, Xishan People's Hospital of Wuxi City, Wuxi, China
[3] Department of Hepatobiliary and Transplantation Surgery, The Affiliated Drum Tower Hospital of Nanjing University Medical School, Nanjing, China
[4] Department of General Surgery, The First Affiliated Hospital of Anhui Medical University, Hefei, China
[*] These authors contributed equally to this work.

ABSTRACT

Background: The severity of liver cirrhosis in hepatocellular carcinoma (HCC) patients is essential for determining the scope of surgical resection. It also affects the long-term efficacy of systemic anti-tumor therapy and transcatheter arterial chemoembolization (TACE). Non-invasive tools, including aspartate aminotransferase to platelet ratio index (APRI), fibrosis-4 (FIB-4), and γ-glutamyl transferase to platelet ratio (GPR), are less accurate in predicting cirrhosis in HCC patients. We aimed to build a novel decision tree model to improve diagnostic accuracy of liver cirrhosis.

Patients and Methods: The Mann-Whitney U test, χ^2 test, and multivariate logistic regression analysis were used to identify independent cirrhosis predictors. A decision tree model was developed using machine learning algorithms in a training cohort of 141 HCC patients. Internal validation was conducted in 99 HCC patients. The diagnostic accuracy and calibration of the established model were evaluated using receiver operating characteristic (ROC) and calibration curves, respectively.

Results: Sex and platelet count were identified as independent cirrhosis predictors. A decision tree model integrating imaging-reported cirrhosis, APRI, FIB-4, and GPR was established. The novel model had an excellent diagnostic performance in the training and validation cohorts, with area under the curve (AUC) values of 0.853 and 0.817, respectively. Calibration curves and the Hosmer-Lemeshow test showed good calibration of the novel model. The decision curve analysis (DCA) indicated that the decision tree model could provide a larger net benefit to predict liver cirrhosis.

Conclusion: Our developed decision tree model could successfully predict liver cirrhosis in HCC patients, which may be helpful in clinical decision-making.

Subjects Gastroenterology and Hepatology, Oncology, Pathology, Radiology and Medical Imaging
Keywords Hepatocellular carcinoma, Liver cirrhosis, Diagnosis, Decision tree model, Machine learning

INTRODUCTION

Primary liver cancer is one of the most prevalent forms of cancer in the world (*Qiu et al., 2022*; *Sauzeau et al., 2022*; *Xu et al., 2022*). It is the fourth most common malignant tumor and the second leading cause of cancer death in China. Hepatocellular carcinoma (HCC) accounts for 75–85% of primary liver cancer (*Craig et al., 2020*; *Sung et al., 2021*). Liver cirrhosis caused by excessive drinking, obesity, hepatitis B virus (HBV) infection, or hepatitis C virus (HCV) infection is an essential contributing factor towards the development of HCC (*Ginès et al., 2021*).

Studies have found that about 1–8% of cirrhotic patients develop HCC yearly (*Ioannou et al., 2007*). HCC incidence also correlates with increased portal pressure or liver stiffness values, which are measured by transient elastography (TE) (*Masuzaki et al., 2009*; *Ripoll et al., 2009*). Radical resection is a vital method for the long-term survival of HCC patients, and the liver reserve function should be carefully evaluated before surgery. Future liver remnant (FLR) of more than 40% is necessary for surgery in cirrhotic patients. Due to the stealthy onset of HCC, less than 30% of patients are suitable for surgical treatment at initial diagnosis (*Zhou et al., 2020*). Local therapy, immunotherapy, and targeted therapy are the main treatments for patients with advanced HCC (*Wang et al., 2022b*). Studies have shown that the degree of liver cirrhosis and liver function status affect the long-term efficacy of systemic anti-tumor therapy and transcatheter arterial chemoembolization (TACE) (*Lencioni et al., 2016*; *Roth et al., 2023*). Therefore, evaluating the level of liver cirrhosis in HCC patients is of great significance.

Liver biopsy (LB) remains the gold standard for cirrhosis assessment. However, the invasive method is expensive and risks serious complications such as bleeding and infection. Sampling error in LB can also lead to an unreliable diagnosis (*Okada et al., 2007*; *Patel & Sebastiani, 2020*). TE is a non-invasive technique used to evaluate liver cirrhosis, but its results are associated with many factors, such as elevated aminotransferase or bilirubin levels, ascites, and extrahepatic cholestasis (*Millonig et al., 2008*; *Yan et al., 2013*). This limits the clinical application of TE in HCC patients. Furthermore, non-invasive tools, including the Child-Pugh (C-P) scoring system, aspartate aminotransferase to platelet ratio index (APRI), and fibrosis-4 (FIB-4), are less accurate in predicting cirrhosis in HCC patients (*Roth et al., 2023*; *Xiao et al., 2016*).

Therefore, we conducted this study intending to establish a new non-invasive model to improve the diagnostic accuracy of cirrhosis in HCC patients.

MATERIALS AND METHODS

Patient selection

We retrospectively reviewed the medical data of HCC patients who underwent curative liver resection at Nanjing Drum Tower Hospital from January 2020 to December 2022. The institutional review board of The Affiliated Drum Tower Hospital of Nanjing University Medical School approved this retrospective study, and the requirement for written informed consent was waived. The STARD 2015 reporting guideline was followed.

Patients with the following conditions were excluded from this study: recurrent HCC; HCC combined with distant metastasis; HCC combined with other tumors; had received local or systemic anti-tumor therapy (targeted therapy or immunotherapy) before surgery; had no des-γ-carboxy prothrombin (DCP) data before surgery. Patients in 2022 were assigned to the training cohort, and patients from 2020 to 2021 were assigned to the validation cohort. Routine laboratory tests were obtained 1 week before surgery, including hepatitis B virus surface antigen (HBsAg), hepatitis C virus antibodies (HCVAb), alpha-fetoprotein (AFP), DCP, red blood cell distribution width (RDW), neutrophil (NE), lymphocyte (LYM), monocyte (M), platelet (PLT), alanine aminotransferase (ALT), aspartate aminotransferase (AST), γ-glutamyl transferase (GGT), total bilirubin (TB), albumin (ALB), C-reactive protein (CRP), prothrombin time (PT), and international normalized ratio (INR). The albumin-bilirubin (ALBI) score is a simple, evidence-based, and objective method of assessing liver function in HCC patients. The ALBI score = $0.66 \times$ log (TB (µmol/L)) − $0.085 \times$ ALB (g/L), and HCC patients were divided into three grades (grade 1: ≤ -2.60; grade 2: > -2.60 to ≤ -1.39; grade 3: > -1.39) according to the scoring results (*Johnson et al., 2015*). The formulas used to calculate inflammatory markers are as follows: GLR = GGT (U/L)/LYM count (10^9/L), PNI = ALB (g/L) + $5 \times$ LYM count (10^9/L), ALRI = AST (U/L)/LYM count (10^9/L), ANRI = AST (U/L)/NE count (10^9/L), SII = PLT count (10^9/L) $\times$ NE count (10^9/L)/LYM count (10^9/L), NLR = NE count (10^9/L)/LYM count (10^9/L), PLR = PLT count (10^9/L)/LYM count (10^9/L), LMR = LYM count (10^9/L)/M count (10^9/L), SIRI = M count (10^9/L) $\times$ NE count (10^9/L)/LYM count (10^9/L) (*Mao et al., 2021*).

Pathological examination

Liver resection specimens were analyzed histologically by two experienced pathologists, who were blinded to the patients' clinical data. Any discrepancy was resolved by their discussion. The liver fibrosis status at the tumor periphery was determined according to the Metavir scoring system. F4 was considered as cirrhosis, F $\geq$ 3 as advanced fibrosis, and F $\geq$ 2 as significant fibrosis (*Bedossa & Poynard, 1996*). Typical pathological section images of F grade 0 to grade 4 were shown in Fig. S1.

Imaging examination

All patients underwent contrast-enhanced computed tomography (CT) or Gd-EOB-DTPA-enhanced magnetic resonance imaging (MRI) within 2 weeks before surgery. Imaging results of all patients were evaluated for cirrhosis by two experienced radiologists. The diagnostic criteria for liver cirrhosis are as follows: the liver has a rough outline, an abnormal proportion of liver lobes, or uneven liver density. Indirect signs of liver cirrhosis include esophageal and gastric varices, ascites, and splenomegaly. Figure S2 presented typical imaging images of liver cirrhosis. Additionally, the maximum tumor diameter was recorded as the mean of two radiologist measurements. The number of tumors was recorded as solitary or multiple (*Yue et al., 2022*). Any discrepancy was resolved by their discussion.

Serum liver cirrhosis diagnostic model

Since PLT, ALT, AST, and GGT are easily obtained parameters, APRI, FIB-4, and γ-glutamyl transferase to platelet ratio (GPR) are commonly used non-invasive diagnostic models of liver fibrosis. The formulas are as follows: FIB-4 = age (years) × AST (U/L)/PLT count (10^9/L) × ALT (U/L)$^{1/2}$; APRI = (AST (U/L)/ULN) × 100/PLT count (10^9/L) (*Itakura et al., 2021*; *Lemoine et al., 2016*).

Statistical analysis and model development

Continuous and categorical variables were compared using the Mann-Whitney U test and χ^2 test, respectively. The subsequent forward conditional multivariate logistic regression analysis (liver cirrhosis status is a binary variable) included variables with $p < 0.10$ in the training cohort (*Katz, 2003*). CT/MRI-reported cirrhosis, independent cirrhosis predictors, APRI, FIB-4, and GPR, were included to establish a novel decision tree using R software (version 3.6.1; *R Core Team, 2019*) and the R package rpart (*Wilson et al., 2018*). Decision tree models are supervised machine learning algorithms widely used in classification and regression tasks due to their interpretability and simplicity. The receiver operating characteristic (ROC) curve and the area under the curve (AUC) value were used to evaluate the diagnostic accuracy of the established decision tree model. The calibration curve was used to evaluate the calibration of the decision tree model, and the Hosmer-Lemeshow test was performed simultaneously (*Dong et al., 2021*; *Li et al., 2022*). Finally, the decision curve analysis (DCA) demonstrated the net clinical benefit at the different thresholds.

RESULTS

Baseline characteristics of enrolled patients

A total of 240 HCC patients were included in this study. There were no significant differences in clinical characteristics between the training cohort (141 patients) and the validation cohort (99 patients) (Table 1). Eighty-three patients (34.5%) were diagnosed with liver cirrhosis by pathological examination (training: 33.3%, 47 of 141; validation: 36.3%, 36 of 99; $p = 0.680$). Figure S3 showed consistency between serum biomarkers (APRI, FIB-4, and GPR) and pathological results.

Risk factors for liver cirrhosis

In the training cohort, except for CT/MRI-reported cirrhosis and three serum diagnostic models (APRI, FIB-4, and GPR), age (years), RDW, LYM, PLT, PT, INR, PNI, ANRI were all related to cirrhosis ($p < 0.05$) (Table 2). Subsequently, the multivariable logistic regression analysis identified sex and PLT count as independent cirrhosis predictive factors ($p < 0.05$) (Table 3 and Fig. S4).

Development and validation of the decision tree model

Since PLT is included in the formulas of APRI, FIB-4, and GPR, we investigated the effect of sex on the diagnostic accuracy of existing models for cirrhosis. The results showed that sex had little effect on diagnostic accuracy (Table 4). In addition, neither imaging nor

Table 1 Baseline characteristics.

Variables	Training (n = 141)	Validation (n = 99)	p value
Basic demographics			
Age (years)	57.0 (51.0–68.0)	57.0 (50.5–67.0)	0.594
Sex			0.322
Male	110	83	
Female	31	16	
BMI (kg/m^2)			0.689
<24	82	61	
≥24	59	38	
Laboratory findings			
HbsAg			0.559
Positive	100	74	
Negative	41	25	
HCVAb			0.326
Positive	4	6	
Negative	137	93	
ALBI grade			0.159
1	91	73	
2 or 3	50	26	
AFP (ng/mL)	22.2 (4.3–139.6)	88.4 (6.2–676.5)	0.139
DCP (mAU/mL)	169.7 (44.4–1,915.3)	369.4 (42.3–2,359.5)	0.606
RDW (%)	12.9 (12.4–13.4)	12.8 (12.4–13.5)	0.710
NE (10^9/L)	3.1 (2.4–3.8)	3.0 (2.3–3.6)	0.723
LYM (10^9/L)	1.5 (1.1–1.8)	1.4 (1.1–1.8)	0.622
M (10^9/L)	0.4 (0.3–0.5)	0.4 (0.3–0.5)	0.859
PLT (10^9/L)	157.0 (110.0–201.0)	149.0 (107.0–181.5)	0.471
ALT (U/L)	25.4 (18.4–36.3)	25.4 (18.3–36.2)	0.437
AST (U/L)	27.0 (21.8–34.3)	26.5 (20.9–37.5)	0.253
GGT (U/L)	44.2 (28.6–74.7)	45.4 (25.6–77.4)	0.432
TB (μmol/L)	13.7 (9.8–16.9)	12.9 (10.1–16.6)	0.883
ALB (g/L)	40.0 (38.7–42.0)	40.6 (39.2–42.5)	0.575
CRP (mg/L)	3.5 (2.1–5.2)	2.8 (2.1–4.8)	0.762
PT (s)	11.3 (10.8–11.8)	11.6 (11.2–11.9)	0.083
INR			0.294
≤1	79	48	
>1	62	51	
Serum fibrosis tests			
APRI	0.5 (0.3–0.7)	0.5 (0.3–0.9)	0.258
FIB-4	2.2 (1.5–3.2)	2.3 (1.5–3.5)	0.456
GPR	0.3 (0.2–0.5)	0.3 (0.2–0.6)	0.413
Inflammatory markers			
GLR	28.9 (17.5–62.6)	30.5 (19.1–56.2)	0.352

(Continued)

Table 1 (continued)

Variables	Training (*n* = 141)	Validation (*n* = 99)	*p* value
PNI	46.7 (43.6–49.7)	46.6 (42.2–50.0)	0.400
ALRI	23.1 (14.2–42.8)	29.9 (17.0–63.2)	0.055
ANRI	10.5 (7.1–16.9)	11.6 (7.1–22.1)	0.091
SII	336.4 (225.0–521.1)	382.5 (237.2–543.6)	0.419
NLR	2.3 (1.7–3.1)	2.5 (1.8–3.5)	0.046
PLR	115.3 (77.9–165.0)	128.8 (86.4–303.8)	0.188
LMR	4.0 (3.3–5.0)	4.0 (3.0–5.0)	0.580
SIRI	0.7 (0.5–1.1)	0.8 (0.5–1.1)	0.721
Pathology parameter			
F			0.680
0–3	94	63	
4	47	36	
Imaging features			
Tumor number			0.928
Solitary	116	81	
Multiple	25	18	
Tumor size (cm)			0.938
≤5	89	62	
>5	52	37	
Cirrhosis			0.691
Present	56	42	
Absent	85	57	

Note:

BMI, body mass index; HbsAg, hepatitis B virus surface antigen; HCVAb, hepatitis C virus antibodies; ALBI, albumin-bilirubin; AFP, alpha-fetoprotein; DCP, des-γ-carboxy prothrombin; RDW, red blood cell distribution width; NE, neutrophil; LYM, lymphocyte; M, monocyte; PLT, platelet; ALT, alanine aminotransferase; AST, aspartate aminotransferase; GGT, γ-glutamyl transferase; TB, total bilirubin; ALB, albumin; CRP, C-reactive protein; PT, prothrombin time; INR, international normalized ratio; APRI, aspartate transaminase to platelet ratio index; FIB-4, fibrosis-4; GPR, γ-glutamyl transferase to platelet ratio; GLR, γ-glutamyl transferase to lymphocyte ratio; PNI, prognostic nutritional index; ALRI, aspartate aminotransferase to lymphocyte ratio index; ANRI, aspartate aminotransferase to neutrophil ratio index; SII, systemic immune-inflammation index; NLR, neutrophil to lymphocyte ratio; PLR, platelet to lymphocyte ratio; LMR, lymphocyte to monocyte ratio; SIRI, systemic inflammation response index.

existing models had an area under the receiver operating characteristic (AUROC) greater than 0.67 in the entire cohort. That is why we intended to establish a novel model to improve the diagnostic accuracy of liver cirrhosis in HCC patients. According to the algorithm, sex was not included in the decision tree. For instance, patients with CT/MRI-reported cirrhosis and FIB-4 ≥ 6.0 are predicted to have cirrhosis, while patients without CT/MRI-reported cirrhosis and APRI < 0.38 are expected not to have cirrhosis (Fig. 1). The decision tree model had excellent diagnostic performance in the training and validation cohorts, with AUROC values of 0.853 (95% CI [0.783–0.923]) and 0.817 (95% CI [0.733–0.902]), respectively (Figs. 2A and 2B). Both calibration curves showed good calibration of the decision tree, indicating that the cirrhosis predicted by the model was consistent with the actual cirrhosis occurrence. The *p*-values of the Hosmer-Lemeshow test were 0.678 and 0.462, respectively (Figs. 2C and 2D). DCA for the decision tree model,

Table 2 Comparisons of clinical characteristics among the training cohort.			
Variables	F 0–3 ($n = 94$)	F 4 ($n = 47$)	p value
Basic demographics			
Age (years)	60.5 (53.0–68.8)	55.0 (50.0–63.5)	0.013
Sex			0.054
Male	78	32	
Female	16	15	
BMI (kg/m^2)			0.718
<24	56	26	
≥24	38	21	
Laboratory findings			
HbsAg			0.078
Positive	62	38	
Negative	32	9	
HCVAb			0.108
Positive	1	3	
Negative	93	44	
ALBI grade			0.062
1	66	25	
2 or 3	28	22	
AFP (ng/mL)	15.4 (3.1–136.9)	41.7 (8.6–176.3)	0.457
DCP (mAU/mL)	236.1 (86.7–2,074.2)	95.7 (32.9–820.5)	0.555
RDW (%)	12.8 (12.4–13.3)	13.1 (12.4–13.5)	0.032
NE (10^9/L)	3.2 (2.6–3.9)	2.9 (2.1–3.6)	0.094
LYM (10^9/L)	1.6 (1.2–2.0)	1.4 (1.0–1.6)	0.010
M (10^9/L)	0.4 (0.3–0.5)	0.3 (0.2–0.5)	0.055
PLT (10^9/L)	176.0 (135.3–208.8)	121.0 (82.5–161.5)	<0.001
ALT (U/L)	25.4 (18.7–36.0)	25.4 (17.8–35.9)	0.660
AST (U/L)	25.1 (20.5–31.3)	32.6 (25.2–40.0)	0.057
GGT (U/L)	45.0 (28.0–68.1)	38.0 (29.7–88.9)	0.579
TB (μmol/L)	13.1 (8.9–16.9)	14.9 (11.8–17.2)	0.178
ALB (g/L)	40.5 (39.1–42.1)	39.5 (38.0–41.8)	0.135
CRP (mg/L)	3.6 (2.1–5.0)	3.2 (2.0–7.9)	0.126
PT (s)	11.1 (10.7–11.6)	11.8 (11.2–12.5)	<0.001
INR			<0.001
≤1	63	16	
>1	31	31	
Serum fibrosis tests			
APRI	0.3 (0.3–0.6)	0.6 (0.5–0.9)	<0.001
FIB-4	1.9 (1.4–2.5)	2.7 (1.8–4.1)	<0.001
GPR	0.3 (0.1–0.4)	0.4 (0.2–0.7)	0.023
Inflammatory markers			
GLR	26.9 (16.3–57.1)	33.1 (21.5–74.3)	0.157

(Continued)

Table 2 (continued)

Variables	F 0–3 (n = 94)	F 4 (n = 47)	p value
PNI	47.4 (43.8–50.3)	45.2 (42.5–47.8)	0.025
ALRI	19.7 (12.5–37.8)	27.7 (21.7–51.3)	0.207
ANRI	8.9 (6.6–14.4)	12.5 (9.0–27.1)	0.004
SII	396.1 (244.6–543.9)	287.7 (161.5–420.9)	0.052
NLR	2.3 (1.7–3.1)	2.3 (1.7–3.1)	0.889
PLR	123.1 (83.2–180.8)	105.0 (75.0–163.1)	0.229
LMR	4.3 (3.4–5.0)	3.8 (3.3–5.2)	0.597
SIRI	0.8 (0.6–1.1)	0.7 (0.4–1.1)	0.608
Imaging features			
Tumor number			0.245
Solitary	80	36	
Multiple	14	11	
Tumor size (cm)			0.268
≤5	56	33	
>5	38	14	
Cirrhosis			<0.001
Present	26	30	
Absent	68	17	

Note:

BMI, body mass index; HbsAg, hepatitis B virus surface antigen; HCVAb, hepatitis C virus antibodies; ALBI, albumin-bilirubin; AFP, alpha-fetoprotein; DCP, des-γ-carboxy prothrombin; RDW, red blood cell distribution width; NE, neutrophil; LYM, lymphocyte; M, monocyte; PLT, platelet; ALT, alanine aminotransferase; AST, aspartate aminotransferase; GGT, γ-glutamyl transferase; TB, total bilirubin; ALB, albumin; CRP, C-reactive protein; PT, prothrombin time; INR, international normalized ratio; APRI, aspartate transaminase to platelet ratio index; FIB-4, fibrosis-4; GPR, γ-glutamyl transferase to platelet ratio; GLR, γ-glutamyl transferase to lymphocyte ratio; PNI, prognostic nutritional index; ALRI, aspartate aminotransferase to lymphocyte ratio index; ANRI, aspartate aminotransferase to neutrophil ratio index; SII, systemic immune-inflammation index; NLR, neutrophil to lymphocyte ratio; PLR, platelet to lymphocyte ratio; LMR, lymphocyte to monocyte ratio; SIRI, systemic inflammation response index.

Table 3 Independent cirrhosis predictive factors in HCC patients.

Variables	Multivariate analysis		
	β	OR	p value
Age (years)	−0.041	0.960 (0.920–1.002)	0.060
Sex	1.016	2.763 (1.007–7.577)	0.048
HbsAg	0.221	1.246 (0.420–3.702)	0.691
ALBI grade	0.479	1.614 (0.124–20.970)	0.714
RDW	0.277	1.319 (0.827–2.104)	0.244
NE	0.211	1.235 (0.727–2.097)	0.434
M	0.133	1.142 (0.037–35.700)	0.940
PLT	−0.016	0.985 (0.971–0.999)	0.032
AST	0.006	1.006 (0.970–1.044)	0.734
PT	0.630	1.877 (0.221–5.925)	0.564
INR	−3.886	0.021 (0.000–0.999)	0.726

Variables	Multivariate analysis		
	β	OR	*p* value
PNI	0.029	1.030 (0.841–1.260)	0.776
ANRI	0.017	1.017 (0.959–1.078)	0.575
SII	0.001	1.001 (0.998–1.004)	0.507

Table 3 (continued)

Note:
HCC, hepatocellular carcinoma; ROC, receiver operating characteristic curve; OR, odds ratio; AUC, area under the curve; HbsAg, hepatitis B virus surface antigen; ALBI, albumin-bilirubin; RDW, red blood cell distribution width; NE, neutrophil; M, monocyte; PLT, platelet; AST, aspartate aminotransferase; PT, prothrombin time; INR, international normalized ratio; PNI, prognostic nutritional index; ANRI, aspartate aminotransferase to neutrophil ratio index; SII, systemic immune-inflammation index.

Table 4 The AUROC and cutoff values of diagnostic tools for liver cirrhosis.

		Entire cohort		
Sex		Male	Female	All
Imaging-reported cirrhosis		0.649 (0.564, 0.734)	0.665 (0.507, 0.823)	0.658 (0.584, 0.731)
APRI	AUROC	0.650 (0.569, 0.731)	0.645 (0.484, 0.805)	0.653 (0.582, 0.724)
	Cutoff	0.47	0.51	0.47
FIB-4	AUROC	0.573 (0.485, 0.661)	0.669 (0.513, 0.826)	0.603 (0.527, 0.678)
	Cutoff	2.39	2.55	2.39
GPR	AUROC	0.585 (0.501, 0.670)	0.577 (0.409, 0.745)	0.577 (0.502, 0.652)
	Cutoff	0.47	0.23	0.43

Note:
AUROC, area under the receiver operating characteristic; APRI, aspartate transaminase to platelet ratio index; FIB-4, fibrosis-4; GPR, γ-glutamyl transferase to platelet ratio.

imaging-reported cirrhosis, APRI, FIB-4, and GPR were presented in Fig. 3, which indicated that the decision tree model provided a larger net benefit than the other four models.

DISCUSSION

Cirrhosis, a late stage of chronic liver inflammation where regenerative cirrhotic nodules replace normal liver structure, can eventually lead to liver failure. About one million people die of liver cirrhosis worldwide annually, and one-third of cirrhotic patients will develop HCC (*Ginès et al., 2021*). Assessment of cirrhosis in patients with chronic liver disease (CLD) or HCC should be the cornerstone of treatment decisions and prognosis (*Patel & Sebastiani, 2020*; *Wang et al., 2022a*).

Radical resection is the best treatment option for HCC patients with Barcelona Clinical Liver Cancer (BCLC) stage 0 or A (*Orimo et al., 2022*). The criteria for assessing the safety of resection are as follows: FLR > 20–30% and indocyanine green (ICG)-R15 < 10% (patients with C-P class A and without liver cirrhosis); FLR > 40% (patients with liver cirrhosis); FLR > 50% and IGG-R15 of 10–20% (patients with liver cirrhosis) (*Zhao & Cai, 2021*). Preoperative evaluation of the liver cirrhosis status of patients is an important basis for determining the scope of surgical resection. For patients within the Milan criteria, liver
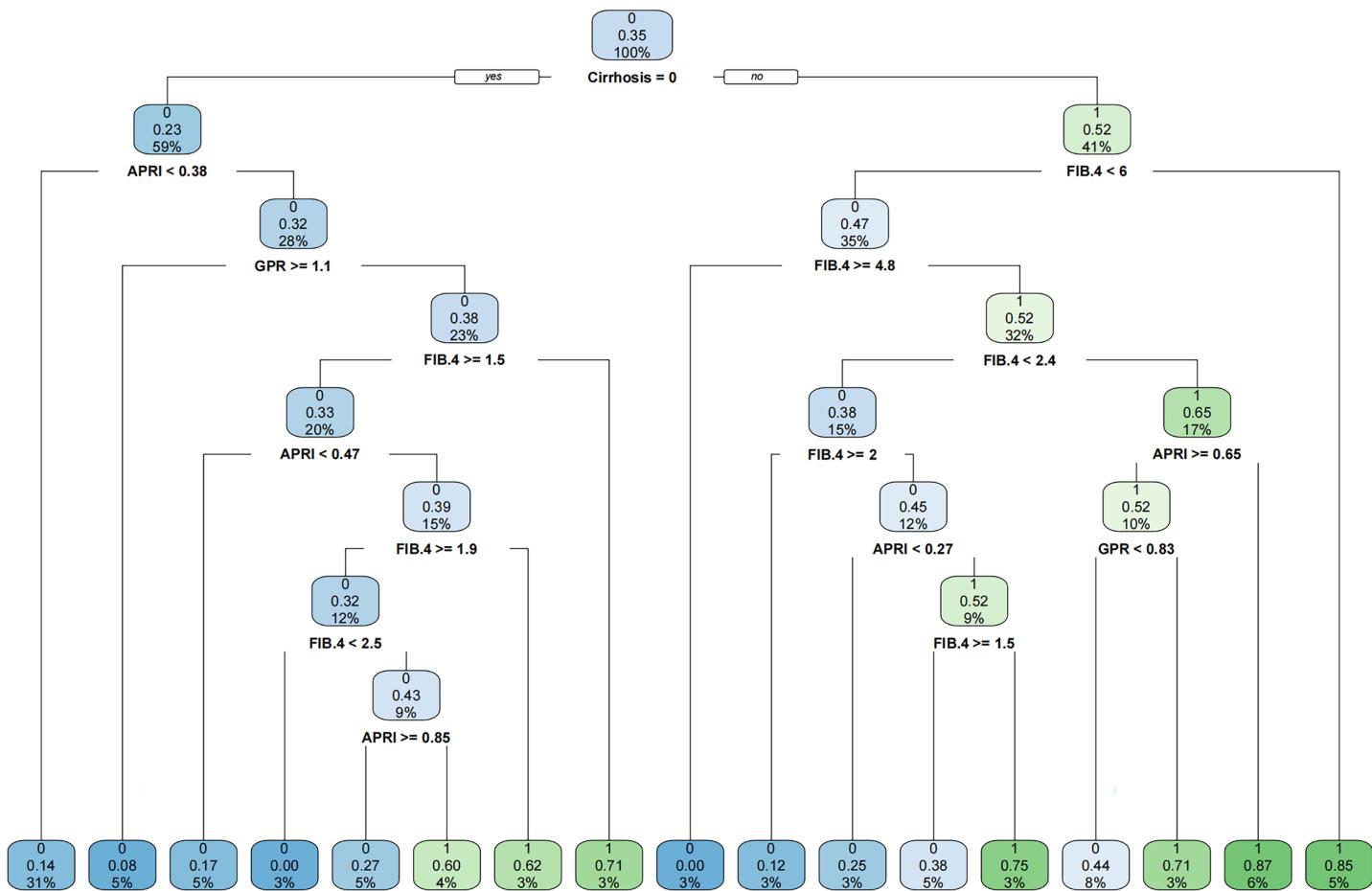
Figure 1 The established novel decision tree model.   Full-size ☑ DOI: 10.7717/peerj.15950/fig-1

transplantation (LT) is recommended as the first-line option for those unsuitable for liver resection (*Marrero et al., 2018*). Liver cirrhosis is a risk factor for postoperative recurrence of HCC (*Marasco et al., 2019*), and cirrhotic patients have a higher risk of developing HCC. Therefore, HCC patients with severe cirrhosis are ideal candidates for LT, accounting for 30–35% of European waiting list patients. Local and systemic treatments are options for HCC patients with BCLC stage B or C. The GIDEON study demonstrated that median overall survival (OS) was longer in C-P class A patients than in C-P class B patients (13.6 months *vs* 5.2 months) (*Marrero et al., 2016*). In addition, the prospective study by *Pressiani et al. (2013)* also showed that the OS and time to progression of C-P class A patients treated with sorafenib were longer than that of C-P class B patients. The C-P scoring system is the most widely used tool for assessing cirrhosis (*Roth et al., 2023*). Hence, assessing liver cirrhosis status in advanced HCC patients can predict treatment efficacy and prognosis. Compensated cirrhosis is asymptomatic, but it can progress to decompensated cirrhosis. Decompensated cirrhosis is associated with various complications (ascites, hepatic encephalopathy, variceal bleeding), leading to poor quality of life and frequent hospitalizations (*Ginès et al., 2021*). Thus, early identification of
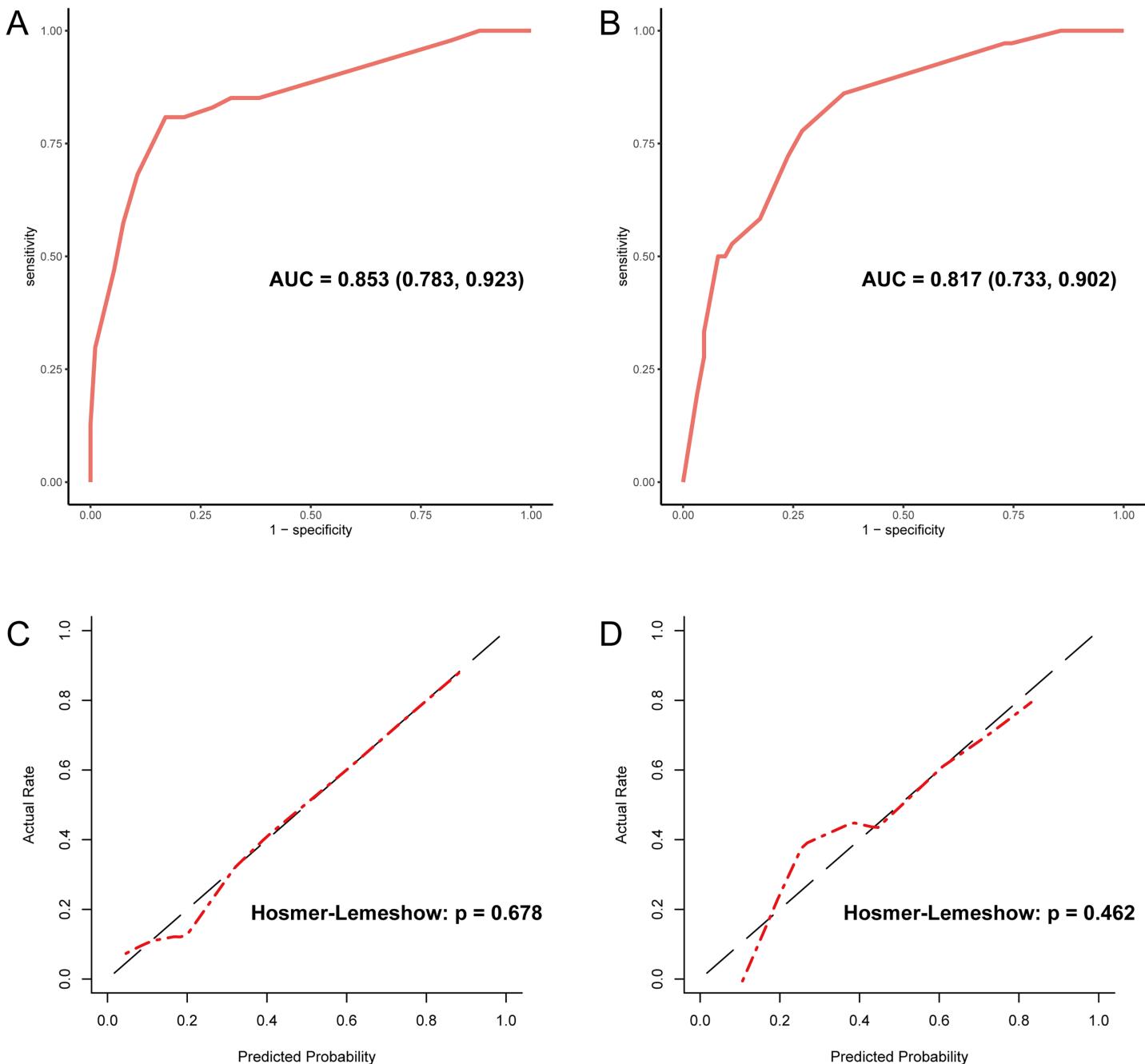
Figure 2 Evaluation of diagnostic accuracy and calibration of the decision tree model. (A) The ROC curve of the training cohort with an AUC value of 0.853. (B) The ROC curve of the validation cohort with an AUC value of 0.817. (C) The calibration curve of the training cohort. (D) The calibration curve of the validation cohort. ROC, receiver operating characteristic; AUC, area under the curve.

Full-size 🖼 DOI: 10.7717/peerj.15950/fig-2

cirrhotic HCC patients for symptomatic and supportive treatment is imperative for mitigating the causative factors and preventing the progression of cirrhosis.

APRI, FIB-4, and GPR include five variables: age, PTL, ATL, AST, and GGT. Age is associated with cirrhosis (*Sterling et al., 2006*), and the incidence of HCC increases with age
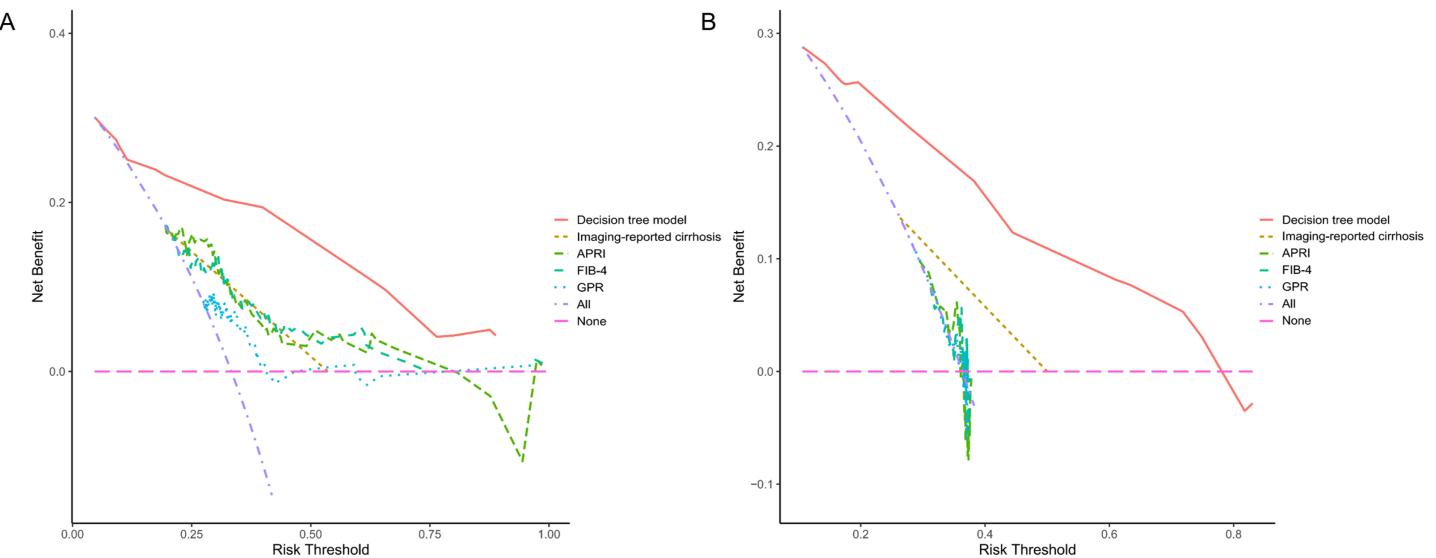
Figure 3 The decision curve analysis for each model in the training (A) and validation (B) cohort. The DCA indicated that the decision tree model could provide a larger net benefit to predict liver cirrhosis. DCA, decision curve analysis; APRI, aspartate transaminase to platelet ratio index; FIB-4, fibrosis-4; GPR, γ-glutamyl transferase to platelet ratio.
Full-size 🖼 DOI: 10.7717/peerj.15950/fig-3
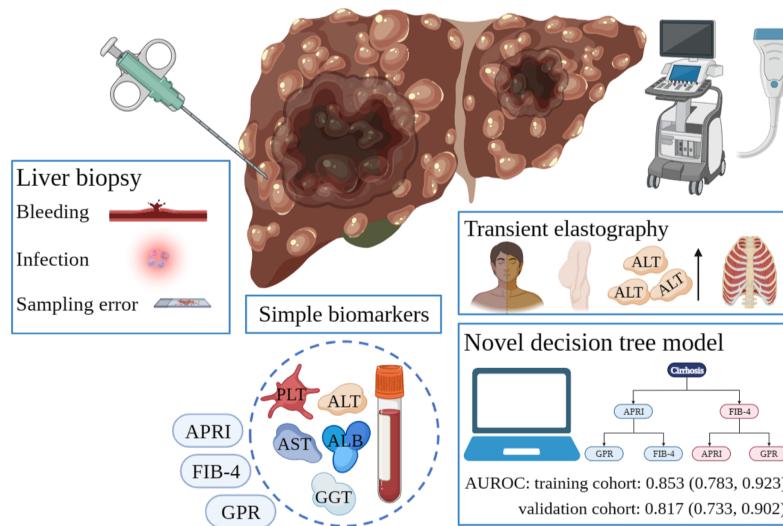
Figure 4 Different diagnostic tools for liver cirrhosis in HCC patients. LB is invasive and risks serious complications such as bleeding and infection. Sampling error in LB can lead to an unreliable diagnosis. Simple serum biomarkers are less accurate. Many factors affecting TE detection results limit its application in HCC patients. Our developed decision tree model can successfully predict liver cirrhosis. HCC, hepatocellular carcinoma; LB, liver biopsy; TE, transient elastography.
Full-size 🖼 DOI: 10.7717/peerj.15950/fig-4

in all populations. Thrombocytopenia occurs in about 78% of patients with liver cirrhosis, and its degree of severity is an early prognostic marker. Decreased thrombopoietin (TPO) levels, hypersplenism secondary to portal hypertension, and myelosuppression induced by antiviral therapy may all lead to decreased PLT (*Peck-Radosavljevic, 2017*). Hepatocellular injury caused by chronic hepatitis can lead to elevated transaminases (especially AST) and

GGT (*Xiao et al., 2016*). To summarize, the variables included in serum diagnostic models correlate with liver fibrosis. The male-to-female ratio of HCC patients is about 2–2.5:1. However, this study found that being female is an independent risk factor for cirrhosis. This may be related to the sample size of the training cohort, which needs to be confirmed by further research.

A previous systematic review and meta-analysis showed that APRI and FIB-4 could identify HBV-related cirrhosis with moderate accuracy and sensitivity (*Xiao, Yang & Yan, 2015*). Meanwhile, *Xiao et al. (2016)* found that the AUC values for APRI and FIB-4 were 0.676 and 0.652 for diagnosing cirrhosis in HBV-related HCC patients. However, *Kim et al. (2016)* proposed that APRI and FIB-4 are unsuitable for evaluating the liver fibrosis of chronic hepatitis B (CHB) patients. This may be because the APRI and FIB-4 models were established in patients with HCV or HCV/HIV co-infection. In summary, the cause of liver cirrhosis and HCC is complicated, and the APRI and FIB-4 models lack high diagnostic accuracy in HCC patients. GPR was established by HBV patients in sub-Saharan African countries, where it was more accurate than APRI or FIB-4 (*Lemoine et al., 2016*). The study by *Lee et al. (2018)* reported that GPR was a valuable marker for assessing the degree of liver fibrosis in CHB patients (AUROC: 0.84; cut-off value: 0.299).

We focused on a noninvasive diagnostic model of cirrhosis status in HCC patients, and resected specimens from all patients were analyzed for liver fibrosis. APRI, FIB-4, and GPR are models established in CLD, and LB is the reference standard. LB specimens account for only 1/50,000 of the liver volume and may not represent the entire liver parenchyma (*Bravo, Sheth & Chopra, 2001*). In addition, LB specimen length (25 mm is considered optimal) and diameter (should be greater than 1 mm) also affect diagnostic accuracy (*Patel & Sebastiani, 2020*). Therefore, using surgical tissues for pathological examination is the advantage of our research. Like existing models, our decision tree model was also developed based on the binary classification of pathological examinations. This may not reflect the dynamic changes of liver fibrosis (*Patel & Sebastiani, 2020*). Although TE can identify liver stiffness in real-time, the Baveno IV consensus suggested that two tests on different days are required to confirm the validity (*de Franchis, 2015*), which will significantly increase the economic burden of HCC patients. Besides, the operator's inexperience is the main factor in the failure of TE detection (*Castéra et al., 2010*). Neither TE nor LB can be used as a routine detection method in areas with limited resources. Abnormal liver function, ascites, narrow intercostal space, obesity, and age over 52 years all affect TE detection (*Castéra et al., 2010*; *Millonig et al., 2008*; *Yan et al., 2013*).

Our research also has some shortcomings. First, selection bias brought about by retrospective research cannot be avoided. Second, there is a lack of external validation cohorts and prospective studies to further assess the model's accuracy. Third, the prevalence situation of HCC in China led us to include mainly HBV-associated patients. Finally, we did not build predictive models for significant and advanced liver fibrosis. This is because radiologists can only evaluate liver cirrhosis, and the diagnosis of cirrhosis is more clinically significant for HCC patients (*Wang et al., 2020*).

CONCLUSIONS

In conclusion, the novel user-friendly decision tree model demonstrated excellent discrimination and calibration in predicting cirrhosis in HCC patients (Fig. 4). Since it is vital to know the cirrhosis status of HCC patients, the model can help clinicians in decision-making.

ADDITIONAL INFORMATION AND DECLARATIONS

Competing Interests

The authors declare that they have no competing interests.

Author Contributions

- Zheyu Zhou conceived and designed the experiments, performed the experiments, analyzed the data, prepared figures and/or tables, authored or reviewed drafts of the article, and approved the final draft.
- Chaobo Chen conceived and designed the experiments, performed the experiments, analyzed the data, prepared figures and/or tables, authored or reviewed drafts of the article, and approved the final draft.
- Meiling Sun conceived and designed the experiments, performed the experiments, analyzed the data, prepared figures and/or tables, authored or reviewed drafts of the article, and approved the final draft.
- Xiaoliang Xu performed the experiments, analyzed the data, prepared figures and/or tables, authored or reviewed drafts of the article, and approved the final draft.
- Yang Liu performed the experiments, analyzed the data, prepared figures and/or tables, authored or reviewed drafts of the article, and approved the final draft.
- Qiaoyu Liu performed the experiments, analyzed the data, prepared figures and/or tables, authored or reviewed drafts of the article, and approved the final draft.

- Jincheng Wang conceived and designed the experiments, performed the experiments, analyzed the data, prepared figures and/or tables, authored or reviewed drafts of the article, and approved the final draft.
- Yin Yin conceived and designed the experiments, authored or reviewed drafts of the article, and approved the final draft.
- Beicheng Sun conceived and designed the experiments, authored or reviewed drafts of the article, and approved the final draft.

Human Ethics

The following information was supplied relating to ethical approvals (*i.e.*, approving body and any reference numbers):

The institutional review board of The Affiliated Drum Tower Hospital of Nanjing University Medical School approved this retrospective study.

Data Availability

The following information was supplied regarding data availability:

The raw data is available in the Supplemental Files.

Supplemental Information

Supplemental information for this article can be found online at http://dx.doi.org/10.7717/peerj.15950#supplemental-information.

REFERENCES

Bedossa P, Poynard T. 1996. An algorithm for the grading of activity in chronic hepatitis C. The METAVIR cooperative study group. *Hepatology* **24**:289–293 DOI 10.1002/(ISSN)1527-3350.

Bravo AA, Sheth SG, Chopra S. 2001. Liver biopsy. *New England Journal of Medicine* **344(7)**:495–500 DOI 10.1056/NEJM200102153440706.

Castéra L, Foucher J, Bernard PH, Carvalho F, Allaix D, Merrouche W, Couzigou P, de Lédinghen V. 2010. Pitfalls of liver stiffness measurement: a 5-year prospective study of 13,369 examinations. *Hepatology* **51**:828–835 DOI 10.1002/hep.23425.

Craig AJ, von Felden J, Garcia-Lezana T, Sarcognato S, Villanueva A. 2020. Tumour evolution in hepatocellular carcinoma. *Nature Reviews Gastroenterology & Hepatology* **17(3)**:139–152 DOI 10.1038/s41575-019-0229-4.

de Franchis R. 2015. Expanding consensus in portal hypertension: report of the Baveno VI consensus workshop: stratifying risk and individualizing care for portal hypertension. *Journal of Hepatology* **63(3)**:743–752 DOI 10.1016/j.jhep.2015.05.022.

Dong S, Yang H, Tang ZR, Ke Y, Wang H, Li W, Tian K. 2021. Development and validation of a predictive model to evaluate the risk of bone metastasis in kidney cancer. *Frontiers in Oncology* **11**:731905 DOI 10.3389/fonc.2021.731905.

Ginès P, Krag A, Abraldes JG, Solà E, Fabrellas N, Kamath PS. 2021. Liver cirrhosis. *The Lancet* **398(10308)**:1359–1376 DOI 10.1016/S0140-6736(21)01374-X.

Ioannou GN, Splan MF, Weiss NS, McDonald GB, Beretta L, Lee SP. 2007. Incidence and predictors of hepatocellular carcinoma in patients with cirrhosis. *Clinical Gastroenterology and Hepatology* **5(8)**:938–945–945.e931–934 DOI 10.1016/j.cgh.2007.02.039.

Itakura J, Kurosaki M, Setoyama H, Simakami T, Oza N, Korenaga M, Tanaka M, Torimura T, Sakamoto N, Enomoto N, Ueno Y, Kawada N, Kaneko S, Nishiguchi S, Chayama K, Tanaka J, Izumi N, Kanto T. 2021. Applicability of APRI and FIB-4 as a transition indicator of liver fibrosis in patients with chronic viral hepatitis. *Journal of Gastroenterology* **56(5)**:470–478 DOI 10.1007/s00535-021-01782-3.

Johnson PJ, Berhane S, Kagebayashi C, Satomura S, Teng M, Reeves HL, O'Beirne J, Fox R, Skowronska A, Palmer D, Yeo W, Mo F, Lai P, Iñarrairaegui M, Chan SL, Sangro B, Miksad R, Tada T, Kumada T, Toyoda H. 2015. Assessment of liver function in patients with hepatocellular carcinoma: a new evidence-based approach-the ALBI grade. *Journal of Clinical Oncology* **33(6)**:550–558 DOI 10.1200/JCO.2014.57.9151.

Katz MH. 2003. Multivariable analysis: a primer for readers of medical research. *Annals of Internal Medicine* **138(8)**:644–650 DOI 10.7326/0003-4819-138-8-200304150-00012.

Kim WR, Berg T, Asselah T, Flisiak R, Fung S, Gordon SC, Janssen HL, Lampertico P, Lau D, Bornstein JD, Schall RE, Dinh P, Yee LJ, Martins EB, Lim SG, Loomba R, Petersen J, Buti M, Marcellin P. 2016. Evaluation of APRI and FIB-4 scoring systems for non-invasive assessment of hepatic fibrosis in chronic hepatitis B patients. *Journal of Hepatology* **64(4)**:773–780 DOI 10.1016/j.jhep.2015.11.012.

Lee J, Kim MY, Kang SH, Kim J, Uh Y, Yoon KJ, Kim HS. 2018. The gamma-glutamyl transferase to platelet ratio and the FIB-4 score are noninvasive markers to determine the severity of liver fibrosis in chronic hepatitis B infection. *British Journal of Biomedical Science* **75(3)**:128–132 DOI 10.1080/09674845.2018.1459147.

Lemoine M, Shimakawa Y, Nayagam S, Khalil M, Suso P, Lloyd J, Goldin R, Njai HF, Ndow G, Taal M, Cooke G, D'Alessandro U, Vray M, Mbaye PS, Njie R, Mallet V, Thursz M. 2016. The gamma-glutamyl transpeptidase to platelet ratio (GPR) predicts significant liver fibrosis and cirrhosis in patients with chronic HBV infection in West Africa. *Gut* **65(8)**:1369–1376 DOI 10.1136/gutjnl-2015-309260.

Lencioni R, de Baere T, Soulen MC, Rilling WS, Geschwind JF. 2016. Lipiodol transarterial chemoembolization for hepatocellular carcinoma: a systematic review of efficacy and safety data. *Hepatology* **64(1)**:106–116 DOI 10.1002/hep.28453.

Li W, Zhou Q, Liu W, Xu C, Tang ZR, Dong S, Wang H, Li W, Zhang K, Li R, Zhang W, Hu Z, Shibin S, Liu Q, Kuang S, Yin C. 2022. A machine learning-based predictive model for predicting lymph node metastasis in patients with Ewing's Sarcoma. *Frontiers in Medicine* **9**:832108 DOI 10.3389/fmed.2022.832108.

Mao S, Yu X, Shan Y, Fan R, Wu S, Lu C. 2021. Albumin-bilirubin (ALBI) and monocyte to lymphocyte ratio (MLR)-based nomogram model to predict tumor recurrence of AFP-negative hepatocellular Carcinoma. *Journal of Hepatocellular Carcinoma* **8**:1355–1365 DOI 10.2147/JHC.S339707.

Marasco G, Colecchia A, Colli A, Ravaioli F, Casazza G, Bacchi Reggiani ML, Cucchetti A, Cescon M, Festi D. 2019. Role of liver and spleen stiffness in predicting the recurrence of hepatocellular carcinoma after resection. *Journal of Hepatology* **70(3)**:440–448 DOI 10.1016/j.jhep.2018.10.022.

Marrero JA, Kudo M, Venook AP, Ye SL, Bronowicki JP, Chen XP, Dagher L, Furuse J, Geschwind JH, de Guevara LL, Papandreou C, Takayama T, Sanyal AJ, Yoon SK, Nakajima K, Lehr R, Heldner S, Lencioni R. 2016. Observational registry of sorafenib use in clinical practice across Child-Pugh subgroups: the GIDEON study. *Journal of Hepatology* **65(6)**:1140–1147 DOI 10.1016/j.jhep.2016.07.020.

Marrero JA, Kulik LM, Sirlin CB, Zhu AX, Finn RS, Abecassis MM, Roberts LR, Heimbach JK. 2018. Diagnosis, staging, and management of hepatocellular carcinoma: 2018 practice guidance by the american association for the study of liver diseases. *Hepatology* **68(2)**:723–750 DOI 10.1002/hep.29913.

Masuzaki R, Tateishi R, Yoshida H, Goto E, Sato T, Ohki T, Imamura J, Goto T, Kanai F, Kato N, Ikeda H, Shiina S, Kawabe T, Omata M. 2009. Prospective risk assessment for hepatocellular carcinoma development in patients with chronic hepatitis C by transient elastography. *Hepatology* **49(6)**:1954–1961 DOI 10.1002/hep.22870.

Millonig G, Reimann FM, Friedrich S, Fonouni H, Mehrabi A, Büchler MW, Seitz HK, Mueller S. 2008. Extrahepatic cholestasis increases liver stiffness (FibroScan) irrespective of fibrosis. *Hepatology* **48(5)**:1718–1723 DOI 10.1002/hep.22577.

Okada T, Sasaki F, Kurauchi N, Kubota M, Itoh T, Honda S, Naito S, Todo S. 2007. Laparoscopic liver biopsy using cup-shaped punch biopsy forceps and argon beam coagulator in children. *Pediatric Surgery International* **23(10)**:947–951 DOI 10.1007/s00383-007-1976-9.

Orimo T, Kamiyama T, Kakisaka T, Nagatsu A, Asahi Y, Aiyama T, Kamachi H, Taketomi A. 2022. Hepatectomy is beneficial in select patients with multiple hepatocellular carcinomas. *Annals of Surgical Oncology* **29(13)**:8436–8445 DOI 10.1245/s10434-022-12495-z.

Patel K, Sebastiani G. 2020. Limitations of non-invasive tests for assessment of liver fibrosis. *JHEP Reports* **2(2)**:100067 DOI 10.1016/j.jhepr.2020.100067.

Peck-Radosavljevic M. 2017. Thrombocytopenia in chronic liver disease. *Liver International* **37(6)**:778–793 DOI 10.1111/liv.13317.

Pressiani T, Boni C, Rimassa L, Labianca R, Fagiuoli S, Salvagni S, Ferrari D, Cortesi E, Porta C, Mucciarini C, Latini L, Carnaghi C, Banzi M, Fanello S, De Giorgio M, Lutman FR, Torzilli G, Tommasini MA, Ceriani R, Covini G, Tronconi MC, Giordano L, Locopo N, Naimo S, Santoro A. 2013. Sorafenib in patients with Child-Pugh class A and B advanced hepatocellular carcinoma: a prospective feasibility analysis. *Annals of Oncology* **24(2)**:406–411 DOI 10.1093/annonc/mds343.

Qiu L, Zhan K, Malale K, Wu X, Mei Z. 2022. Transcriptomic profiling of peroxisome-related genes reveals a novel prognostic signature in hepatocellular carcinoma. *Genes & Diseases* **9(1)**:116–127 DOI 10.1016/j.gendis.2020.04.010.

R Core Team. 2019. *R: A language and environment for statistical computing*. Version 3.6.1. Vienna: R Foundation for Statistical Computing. *Available at* https://www.r-project.org.

Ripoll C, Groszmann RJ, Garcia-Tsao G, Bosch J, Grace N, Burroughs A, Planas R, Escorsell A, Garcia-Pagan JC, Makuch R, Patch D, Matloff DS. 2009. Hepatic venous pressure gradient predicts development of hepatocellular carcinoma independently of severity of cirrhosis. *Journal of Hepatology* **50(5)**:923–928 DOI 10.1016/j.jhep.2009.01.014.

Roth GS, Villeret F, Decaens T, Merle P, Nahon P. 2023. Immunotherapy in hepatocellular carcinoma: how does underlying liver disease influence therapeutic strategy and outcomes? *Liver International* **43(3)**:546–557 DOI 10.1111/liv.15504.

Sauzeau V, Beignet J, Vergoten G, Bailly C. 2022. Overexpressed or hyperactivated Rac1 as a target to treat hepatocellular carcinoma. *Pharmacological Research* **179**:106220 DOI 10.1016/j.phrs.2022.106220.

Sterling RK, Lissen E, Clumeck N, Sola R, Correa MC, Montaner J, Sulkowski MS, Torriani FJ, Dieterich DT, Thomas DL, Messinger D, Nelson M. 2006. Development of a simple noninvasive index to predict significant fibrosis in patients with HIV/HCV coinfection. *Hepatology* **43**:1317–1325 DOI 10.1002/(ISSN)1527-3350.

Sung H, Ferlay J, Siegel RL, Laversanne M, Soerjomataram I, Jemal A, Bray F. 2021. Global cancer statistics 2020: GLOBOCAN estimates of incidence and mortality worldwide for 36 cancers in 185 countries. *CA: A Cancer Journal for Clinicians* **71(3)**:209–249 DOI 10.3322/caac.21660.

Wang JC, Fu R, Tao XW, Mao YF, Wang F, Zhang ZC, Yu WW, Chen J, He J, Sun BC. 2020. A radiomics-based model on non-contrast CT for predicting cirrhosis: make the most of image data. *Biomarker Research* **8(1)**:47 DOI 10.1186/s40364-020-00219-y.

Wang J, Tang S, Mao Y, Wu J, Xu S, Yue Q, Chen J, He J, Yin Y. 2022a. Radiomics analysis of contrast-enhanced CT for staging liver fibrosis: an update for image biomarker. *Hepatology International* **16(3)**:627–639 DOI 10.1007/s12072-022-10326-7.

Wang J, Wu R, Sun JY, Lei F, Tan H, Lu X. 2022b. An overview: management of patients with advanced hepatocellular carcinoma. *BioScience Trends* **16(6)**:405–425 DOI 10.5582/bst.2022.01109.

Wilson TJ, Howe BM, Stewart SA, Spinner RJ, Amrami KK. 2018. Clinicoradiological features of intraneural perineuriomas obviate the need for tissue diagnosis. *Journal of Neurosurgery* **129(4)**:1034–1040 DOI 10.3171/2017.5.JNS17905.

Xiao G, Yang J, Yan L. 2015. Comparison of diagnostic accuracy of aspartate aminotransferase to platelet ratio index and fibrosis-4 index for detecting liver fibrosis in adult patients with chronic hepatitis B virus infection: a systemic review and meta-analysis. *Hepatology* **61(1)**:292–302 DOI 10.1002/hep.27382.

Xiao G, Zhu F, Wang M, Zhang H, Ye D, Yang J, Jiang L, Liu C, Yan L, Qin R. 2016. Diagnostic accuracy of APRI and FIB-4 for predicting hepatitis B virus-related liver fibrosis accompanied with hepatocellular carcinoma. *Digestive and Liver Disease* **48(10)**:1220–1226 DOI 10.1016/j.dld.2016.06.001.

Xu M, Yang L, Lin Y, Lu Y, Bi X, Jiang T, Deng W, Zhang L, Yi W, Xie Y, Li M. 2022. Emerging nanobiotechnology for precise theranostics of hepatocellular carcinoma. *Journal of Nanobiotechnology* **20(1)**:427 DOI 10.1186/s12951-022-01615-2.

Yan LB, Zhu X, Bai L, Liang LB, Chen EQ, Du LY, Wang LC, Chen LY, Tang H. 2013. Impact of mild to moderate elevations of alanine aminotransferase on liver stiffness measurement in chronic hepatitis B patients during antiviral therapy. *Hepatology Research* **43(2)**:185–191 DOI 10.1111/j.1872-034X.2012.01068.x.

Yue Q, Zhou Z, Zhang X, Xu X, Liu Y, Wang K, Liu Q, Wang J, Zhao Y, Yin Y. 2022. Contrast-enhanced CT findings-based model to predict MVI in patients with hepatocellular carcinoma. *Bmc Gastroenterology* **22(1)**:544 DOI 10.1186/s12876-022-02586-2.

Zhao HT, Cai JQ. 2021. Chinese expert consensus on neoadjuvant and conversion therapies for hepatocellular carcinoma. *World Journal of Gastroenterology* **27(47)**:8069–8080 DOI 10.3748/wjg.v27.i47.8069.

Zhou J, Sun H, Wang Z, Cong W, Wang J, Zeng M, Zhou W, Bie P, Liu L, Wen T, Han G, Wang M, Liu R, Lu L, Ren Z, Chen M, Zeng Z, Liang P, Liang C, Chen M, Yan F, Wang W, Ji Y, Yun J, Cai D, Chen Y, Cheng W, Cheng S, Dai C, Guo W, Hua B, Huang X, Jia W, Li Y, Li Y, Liang J, Liu T, Lv G, Mao Y, Peng T, Ren W, Shi H, Shi G, Tao K, Wang W, Wang X, Wang Z, Xiang B, Xing B, Xu J, Yang J, Yang J, Yang Y, Yang Y, Ye S, Yin Z, Zhang B, Zhang B, Zhang L, Zhang S, Zhang T, Zhao Y, Zheng H, Zhu J, Zhu K, Liu R, Shi Y, Xiao Y, Dai Z, Teng G, Cai J, Wang W, Cai X, Li Q, Shen F, Qin S, Dong J, Fan J. 2020. Guidelines for the diagnosis and treatment of hepatocellular carcinoma (2019 edition). *Liver Cancer* **9(6)**:682–720 DOI 10.1159/000509424.